

## Facile Construction of Lanthanide Metallomacrocycles with the Bridging Imidazolate and Triazolate Ligands and Their Ring Expansions

Jie Zhang,\* Ruifang Cai, Zhenxia Chen, and Xigeng Zhou\*

Department of Chemistry, Fudan University, Shanghai 200433, People's Republic of China

Received September 11, 2006

Four novel tri- or tetranuclear organolanthanide metallomacrocycles  $[Cp_2Ln(\mu\text{-Im})(THF)_3]$  ( $Cp = C_5H_5$ ,  $Ln = Yb$  (**1**),  $Er$  (**2**)),  $[Cp_2Dy(\mu\text{-Im})_4(THF)]_4\cdot2THF$  (**3**), and  $[Cp'_2Yb(\mu\text{-}\eta^1\text{-}\eta^2\text{-Tz})_4\cdot2THF$  ( $Cp' = CH_3C_5H_4$ ) (**4**) have been synthesized through protolysis of  $Cp_3Ln$  or  $Cp'_3Yb$  with imidazole or triazole, indicating that both the bridge-ligand size and the lanthanide-ion radii can be applied in the modulation of the metallomacrocycles. Further investigations on the reactivity of complexes **1**, **3**, and **4** toward phenyl isocyanate reveal that PhNCO inserts readily into the simple bridge  $Ln\text{-N}$  bonds of **1** and **3** to yield the corresponding insertion products  $[Cp_2Ln(\mu\text{-}\eta^1\text{-}\eta^2\text{-OC(Im)NPh})_3]$  ( $Ln = Yb$  (**5**),  $Dy$  (**6**)) but cannot insert into the  $Ln\text{-N}$  bond with a  $\mu\text{-}\eta^1\text{-}\eta^2$ -bonding mode in **4**. The novel bridge ligand  $[OC(Im)NPh]$  can expand the numbers of the ring members from 12 to 18 in **5** or 16 to 18 in **6**. The number of metal atoms in the metallacycles with the ligand  $[OC(Im)NPh]$  is independent of the lanthanide-ion size; both trinuclear lanthanide macrocycles are observed in **5** and **6**. All of these new complexes have been characterized by elemental analysis and spectroscopic properties, and their structures have also been determined through X-ray single-crystal diffraction analysis.

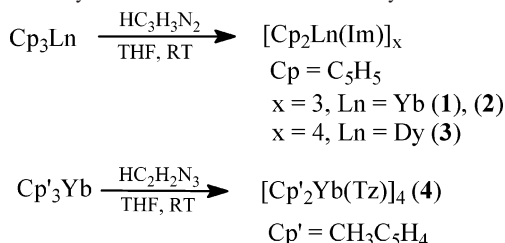
### Introduction

Great interest has been focused on the rapidly expanding field of supramolecular chemistry because these systems can be widely used in molecular recognition,<sup>1</sup> selective transformations,<sup>2</sup> translocation of drugs across membranes,<sup>3</sup> and construction of macroscopic architectures and devices on the molecular level.<sup>4</sup> Many organometallic macrocyclic com-

plexes have been synthesized as important building blocks for construction of functional supramolecular materials by use of the “molecular library” model in recent decades.<sup>5,6</sup> However, organolanthanide macrocycles have been scarcely reported.<sup>7</sup> It can be partly attributed to the fact that lantha-

- \* To whom correspondence should be addressed. E-mail: zhangjie@fudan.edu.cn (J.Z.); xgzhou@fudan.edu.cn (X.Z.).
- (1) (a) Yoshizawa, M.; Kusukawa, T.; Fujita, M.; Yamaguchi, K. *J. Am. Chem. Soc.* **2000**, *122*, 6311. (b) Sun, S. S.; Lees, A. J. *J. Am. Chem. Soc.* **2000**, *122*, 8956. (c) Fujita, M.; Fujita, N.; Ogura, K.; Yamaguchi, K. *Nature* **1999**, *400*, 52. (d) Ikeda, A.; Yoshimura, M.; Uduz, H.; Fukuhara, C.; Shinkai, S. *J. Am. Chem. Soc.* **1999**, *121*, 4296. (e) Hiraoka, S.; Fujita, M. *J. Am. Chem. Soc.* **1999**, *121*, 10239. (f) Jeong, K. S.; Cho, Y. L.; Song, J. U.; Chang, H. Y.; Choi, M. G. *J. Am. Chem. Soc.* **1998**, *120*, 10982. (g) Fujita, M.; Nagao, S.; Ogura, K. *J. Am. Chem. Soc.* **1995**, *117*, 1649. (h) Slone, R. V.; Yoon, D. I.; Calhoun, R. M.; Hupp, J. T. *J. Am. Chem. Soc.* **1995**, *117*, 11813.
- (2) (a) Kang, J.; Santamaris, J.; Hilmersson, G.; Rebek, J., Jr. *J. Am. Chem. Soc.* **1998**, *120*, 7389. (b) Kang, J.; Hilmersson, G.; Santamaris, J.; Rebek, J., Jr. *J. Am. Chem. Soc.* **1998**, *120*, 3650. (c) Kang, J.; Hilmersson, G.; Santamaris, J.; Rebek, J., Jr. *Nature* **1997**, *385*, 50. (d) Walter, C. J.; Anderson, H. L.; Sanders, J. K. M. *J. Chem. Soc., Chem. Commun.* **1993**, 458.
- (3) (a) Keefe, M. H.; Slone, R. V.; Hupp, J. T.; Czaplewski, K. F.; Snurr, R. Q.; Stern, C. L. *Langmuir* **2000**, *16*, 3964. (b) Belanger, S.; Hupp, J. T. *Angew. Chem., Int. Ed.* **1999**, *38*, 2222. (c) Belanger, S.; Hupp, J. T.; Stern, C. L.; Slone, R. V.; Watson, D. F.; Carrell, T. G. *J. Am. Chem. Soc.* **1999**, *121*, 557.

- (4) (a) Holiday, B. J.; Mirkin, C. A. *Angew. Chem., Int. Ed.* **2001**, *40*, 2202. (b) Balzani, V.; Credi, A.; Raymo, F. M.; Stoddart, J. F. *Angew. Chem., Int. Ed.* **2000**, *39*, 3348. (c) Lent, C. S. *Science* **2000**, *288*, 1597. (d) Pineri, R. D.; Zhu, J.; Xu, F.; Hong, S.; Mirkin, C. A. *Science*, **1999**, *283*, 661. Xia, Y.; Whitesides, G. M. *Angew. Chem., Int. Ed.* **1998**, *37*, 550.
- (5) (a) Swiegers, G. F.; Malefetse, T. J. *Coord. Chem. Rev.* **2002**, *225*, 91. (b) Cotton, F. A.; Lin, C.; Murillo, C. A. *Acc. Chem. Res.* **2001**, *34*, 759. (c) Leininger, S.; Olenyuk, B.; Stang, P. J. *Chem. Rev.* **2000**, *100*, 853. (d) Swiegers, G. F.; Malefetse, T. J. *Chem. Rev.* **2000**, *100*, 3484.
- (6) (a) Jude, H.; Disteldorf, H.; Fischer, S.; Wedge, T.; Hawkridge, A. M.; Arif, A. M.; Hawthorne, M. F.; Muddiman, D. C.; Stang, P. J. *J. Am. Chem. Soc.* **2005**, *127*, 12131. (b) Wang, P.; Moorefield, C. N.; Newkome, G. R. *Angew. Chem., Int. Ed.* **2005**, *44*, 1679. (c) Grote, Z.; Scopelliti, R.; Severin, K. *J. Am. Chem. Soc.* **2004**, *126*, 16959. (d) Kraft, S.; Beckhaus, R.; Hasse, D.; Saak, W. *Angew. Chem., Int. Ed.* **2004**, *43*, 1583. (e) Angaridis, P.; Berry, J. F. B.; Cotton, F. A.; Murillo, C. A.; Wang, X. *J. Am. Chem. Soc.* **2003**, *125*, 10327. (e) Benkstein, K. D.; Hupp, J. T.; Stern, C. L. *Angew. Chem., Int. Ed.* **2000**, *39*, 2891. (f) Lai, S. W.; Chan, M. C. W.; Peng, S. M.; Che, C. M. *Angew. Chem., Int. Ed.* **1999**, *38*, 669. (g) Benkstein, K. D.; Hupp, J. T.; Stern, C. L. *J. Am. Chem. Soc.* **1998**, *120*, 12982.
- (7) (a) Anwander, R. *Angew. Chem., Int. Ed.* **1998**, *37*, 599 and references therein. (b) Zhao, B.; Li, H.; Shen, Q.; Zhang, Y.; Yao, Y.; Lu, C. *Organometallics* **2006**, *25*, 1824.

**Scheme 1.** Synthesis of the Lanthanide Metallacycles

nide-metal ions have higher coordination numbers (8–12) than transition-metal ions (4 or 6), thus increasing the inscrutability of self-assembled structure.<sup>8</sup> Furthermore, construction of suitable macrocyclic systems containing transition metals usually can be achieved solely by optimizing steric factors through varying the co- or bridge-ligand size. However, for the lanthanide metals, there is an additional opportunity to optimize steric factors by varying the size of the metal atom themselves because the limited radial extension of 4f valence orbitals makes these metals chemically similar and there are 15 choices.<sup>9</sup> Our interest is to investigate the effect of the lanthanide-metal ion size and different bridging ligands on construction of lanthanide-metal-based macrocycles. In this contribution, we report the synthesis and crystal structures of novel lanthanocene macrocycles with bridging imidazolate and triazolate ligands, determining whether larger ion radii and M–L–M angles are favorable for formation of larger metallomacrocycles. Further study reveals that metallacycle ring expansions can be achieved through insertion of phenyl isocyanate to the M–N(Im) bond.

## Results and Discussion

**Synthesis and Characterizations of Lanthanide Metallacycles 1–4.** The protolysis reaction is a useful method for the synthesis of lanthanocene derivatives containing aromatic N-heterocycle ligands due to the acidity of the hydrogen atom on the nitrogen atom in these ligands.<sup>10</sup> We first investigated the protolysis reaction of  $\text{Cp}_3\text{Ln}$  ( $\text{Cp} = \text{C}_5\text{H}_5$ ) with 1 equiv of imidazole (HIm) in THF at room temperature, giving trinuclear cyclic complexes  $[\text{Cp}_2\text{Ln}(\mu\text{-Im})]_3$  ( $\text{Ln} = \text{Yb (1), Er (2)}$ ) in high yields, which are moderately soluble in THF, as shown in Scheme 1.

Single crystals suitable for X-ray diffraction analysis were isolated by recrystallization of **1** and **2** from THF at  $-20^\circ\text{C}$  for several days, and their structures are shown in Figure 1, determined by X-ray crystallography. Complexes **1** and **2** are isostructural with the solvent-free trimer. Unfortunately, the quality of the crystallographic data for **1** is poor (but

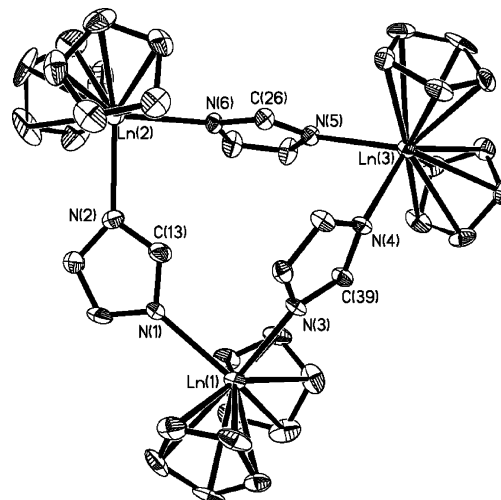


**Figure 1.** Molecular drawing and X-ray crystal structure of  $[\text{Cp}_2\text{Ln}(\mu\text{-Im})]_3$  ( $\text{Ln} = \text{Yb (1), Er (2)}$ ), showing the atom-numbering scheme. Anisotropic thermal displacement ellipsoids are shown at the 30% probability level.

sufficient to provide atom connectivity); only the bond distances and bond angles for **2** are discussed. In **2**, each erbium atom is coordinated by two  $\eta^5\text{-Cp}$  rings and two nitrogen atoms from two imidazolate ligands with a distorted tetrahedron geometry. The three erbium centers are linked together through three deprotonated imidazole bridging ligands, forming a neutral 12-membered metallacycle with alternating imidazolates and erbiums. There are substantial differences between the C–N bond lengths of the imidazolate ligands of **2** and the free imidazole molecule. The crystal structure of the free imidazole shows two different C–N bond lengths of 1.349(4) and 1.326(6) Å.<sup>11</sup> In the ligated imidazolates of **2**, however, the two C–N bond lengths are approximately equal with a mean value of 1.297(11) Å (N(1)–C(13) 1.294(11) Å, N(2)–C(13) 1.299(11) Å), slightly smaller than the corresponding values of the free imidazole. This can be explained in terms of  $\pi$  delocalization owing to deprotonation of the bridging ligand. Consistent with this observation, the Er(1)–N(1) and Er(2)–N(2) distances, 2.341(7) and 2.325(7) Å, are also approximately equal and intermediate between the values observed for the Ln–N single-bond distance and the Ln–N donor bond distance.<sup>12</sup>

In our previous study we found that reaction of  $\text{Cp}_3\text{Ln}$  with the pyrazole only formed monomer or dimer lanthanide complexes.<sup>13</sup> This may be attributed to the pyrazolate ligands having a smaller M–L–M angle. The imidazolate ligand is favorable for binding to metal ions, is an excellent bridging ligand, and has been extensively investigated in transition-organometallic complexes and inorganic coordination poly-

- (8) (a) Arndt, S.; Okunda, J. *Chem. Rev.* **2002**, *102*, 1953. (b) Schumann, H.; Meese-Markscheffel, J. A.; Esser, L. *Chem. Rev.* **1995**, *95*, 865.
- (c) Evans, W. J.; Drummond, D. K.; Grate, J. W.; Zhang, H. M.; Atwood, J. L. *J. Am. Chem. Soc.* **1987**, *109*, 3928.
- (9) (a) Freeman, A. J.; Watson, R. E. *Phys. Rev.* **1976**, *9*, 217. (b) Moeller, T. In *Comprehensive Inorganic Chemistry*; Bailar, J. C., Ed.; Pergamon Press: Oxford, 1973; Vol. 4, Chapter 44. (c) Evans, W. J.; Nyce, G. W.; Clark, R. D.; Doedens, R. J.; Ziller, J. W. *Angew. Chem., Int. Ed.* **1999**, *38*, 1801. (d) Evans, W. J.; Gonzales, S. L.; Ziller, J. W. *J. Am. Chem. Soc.* **1991**, *113*, 7423.
- (10) (a) Ma, L. P.; Zhang, J.; Cai, R. F.; Chen, Z. X.; Weng, L. H.; Zhou, X. G. *J. Organomet. Chem.* **2005**, *690*, 4962. (b) Zhang, J.; Cai, R. F.; Weng, L. H.; Zhou, X. G. *Organometallics* **2003**, *22*, 5385.

- (11) Sagrario, M. C. *Acta Crystallogr.* **1966**, *20*, 783.
- (12) (a) Zhang, J.; Cai, R. F.; Weng, L. H.; Zhou, X. G. *Dalton Trans.* **2006**, *1168*. (b) Zhang, J.; Ma, L. P.; Cai, R. F.; Weng, L. H.; Zhou, X. G. *Organometallics* **2005**, *24*, 738. (c) Zhang, J.; Zhou, X. G.; Cai, R. F.; Weng, L. H. *Inorg. Chem.* **2005**, *44*, 716. (d) Zhang, J.; Cai, R. F.; Weng, L. H.; Zhou, X. G. *Organometallics* **2004**, *23*, 3303. (e) Zhang, J.; Ruan, R. Y.; Shao, Z. H.; Cai, R. F.; Weng, L. H.; Zhou, X. G. *Organometallics* **2002**, *21*, 1420.
- (13) (a) Zhou, X. G.; Huang, Z. E.; Cai, R. F.; Zhang, L. B.; Zhang, L. X.; Huang, X. Y. *Organometallics* **1999**, *18*, 4128. (b) Zhou, X. G.; Zhang, L. B.; Ruan, R. Y.; Zhang, L. X.; Cai, R. F.; Weng, L. H. *Chin. Sci. Bull.* **2001**, *46*, 723.

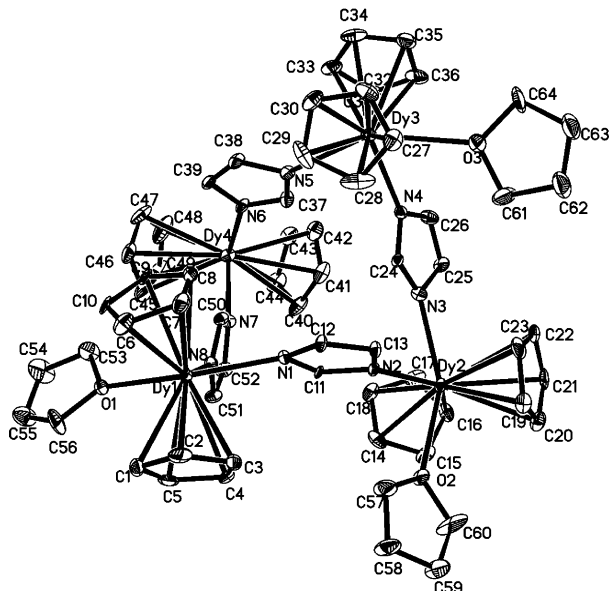


**Figure 2.** Molecular drawing and X-ray crystal structure of  $[Cp_2Dy(\mu\text{-Im})_4(THF)_3 \cdot 2THF]$  (**3**), showing the atom-numbering scheme. Anisotropic thermal displacement ellipsoids are shown at the 30% probability level.

mers.<sup>14</sup> However, knowledge about their rare-earth-metal complexes is rather limited; only a few lanthanide complexes with imidazolate ligands have been synthesized to date.<sup>15</sup> We first introduce the bridging imidazolate ligand into the organolanthanide chemistry to construct lanthanide macrocycles. Interestingly, reaction of  $Cp_3Dy$  with the imidazole under the same conditions gave a tetranuclear cyclic product  $[(C_5H_5)_2Dy(\mu\text{-Im})_4(THF)_3 \cdot 2THF]$  (**3**) in 74% yield, probably owing to the larger ionic radius of  $Dy^{3+}$  than that of  $Er^{3+}$ . These results may be indicative of the metal atom number of these multinuclear compounds being manipulated through programmed variation of the lanthanide metal ions, and the lanthanide metal can provide another opportunity to design metallocycles. X-ray diffraction analysis (Figure 2) reveals that the coordination mode of the metal centers and the imidazolate ligands in **3** is similar to that of **2**. A unique characteristic of **3** is that the four dysprosium centers are not coplanar and form a butterfly-type structure, which is significantly different from the analogous transition-metal complex  $[\text{Fe}(\text{NO})_2(\mu\text{-Im})_4]$  of which the four iron centers are approximately coplanar.<sup>16</sup> This can be attributed to the fact that the lanthanide-metal ions need higher coordinated numbers (the THF molecules are also coordinated to the metal centers). Significantly, three THF molecules are closed

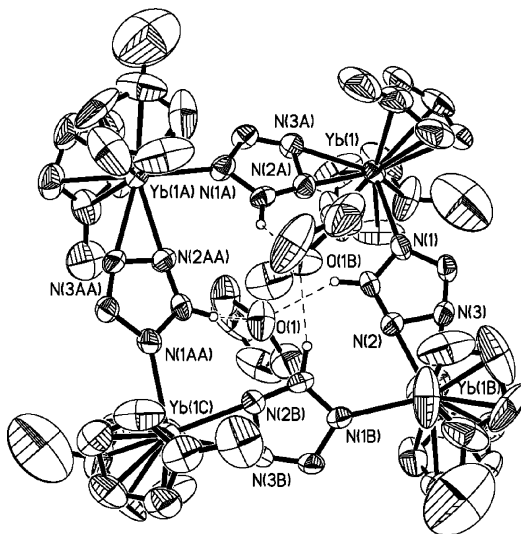


**Figure 3.** Molecular drawing and X-ray crystal structure of  $[Cp'_2Yb(\mu\text{-}\eta^1\text{-}\eta^2\text{-Tz})_4 \cdot 2THF]$  (**4**), showing the atom-numbering scheme. Anisotropic thermal displacement ellipsoids are shown at the 30% probability level (high thermal ellipsoids of some carbon atoms in the  $Cp'$  rings or THF).

to the three dysprosium centers, two other THF molecules only exist in the crystal lattice, and not coordinated to the fourth  $Dy^{3+}$  ion. The coordination environment around the metal centers reduces the structural symmetry of **3**. It should be noted that poor solubility caused problems when we extended our study to other lanthanide elements with larger ion radii. For example, the products of the reaction of  $Cp_3Nd$  with imidazole are sparingly soluble in THF, and its solid-state structure cannot be obtained.

In order to investigate the effect of the bridging ligand on construction of lanthanide metallocycles, reaction of  $Cp'_3Ln$  ( $Cp' = CH_3C_5H_4$ ) with triazole (HTz) has also been studied. The M–L–M angle of the triazolate ligand is almost  $180^\circ$  and larger than that of the imidazolate ligand. Reaction of  $Cp'_3Yb$  with 1 equiv of triazole in THF at room temperature gave the THF-soluble tetranuclear square-planar metallocycle  $[Cp'_2Yb(\mu\text{-}\eta^1\text{-}\eta^2\text{-Tz})_4 \cdot 2THF]$  (**4**) in 78% yield. It should be noted that the analogous metallocycle with unsubstituted  $Cp$  ligands ( $Cp = C_5H_5$ ) instead of the supporting  $Cp'$  ligands is not soluble in THF, and we cannot obtain single crystals suitable for X-ray diffraction analysis. **4** crystallizes in a cubic  $I-43d$  space group with 12 molecules per unit cell. Each ytterbium center had two  $\eta^5$ - $Cp'$  ligands and three nitrogen atoms, two from one triazolate ligand and one from another triazolate ligand. The four ytterbium centers are linked together through four deprotonated triazole bridging ligands, forming a neutral 16-membered approximately square-planar macrocycle. The dihedral angle between the planes of  $Yb(1)\text{-}Yb(1A)\text{-}Yb(1B)$  and  $Yb(1)\text{-}Yb(1B)\text{-}Yb(1C)$  is  $163.0^\circ$ , significantly different from that of **3**. This should be attributed to the coordinated  $\mu\text{-}\eta^1\text{-}\eta^2$ -mode of the triazolate ligand to the  $Yb^{3+}$  ions. More interestingly, the two uncoordinated THF molecules not only exist in the crystal lattice, but also bond to the macrocycle through a novel intermolecular  $\mu\text{-}\eta^2\text{-}C\text{-}H\cdots O$  hydrogen bond with the inboard C–H bonds of the four triazolate ligands, as shown in Figure 4. Hydrogen

(14) (a) Tian, Y. Q.; Cai, C. X.; Ji, Y.; You, X. Z.; Peng, S. M.; Lee, G. H. *Angew. Chem., Int. Ed.* **2002**, *41*, 1384. (b) Perera, J. R.; Heeg, M. J.; Winter, C. H. *Organometallics* **2000**, *19*, 5263. (c) Ohtsu, H.; Shimazaki, Y.; Odani, A.; Yamachio, O.; Mori, W.; Itoh, S.; Fukuzumi, S. *J. Am. Chem. Soc.* **2000**, *122*, 5733. (d) Rettig, S. J.; Storr, A.; Summers, D. A.; Thompson, R. C.; Trotter, J. *J. Am. Chem. Soc.* **1997**, *119*, 8675. (e) Pierre, J. L.; Chautemps, P.; Refaïf, S.; Beguin, C.; Marzouki, A. E.; Serratrice, G.; Saint-Aman, E.; Rey, P. *J. Am. Chem. Soc.* **1995**, *117*, 1965.

(15) (a) Zhang, Z. H.; Song, Y.; Okamura, T.; Hasegawa, Y.; Sun, W. Y.; Ueyama, N. *Inorg. Chem.* **2006**, *45*, 2896. (b) Sun, C. Y.; Kang, B. S.; Mu, X. Q.; Sun, J.; Tong, Y. X.; Chen, Z. N. *Aust. J. Chem.* **1998**, *51*, 565.

(16) Wang, X.; Sundberg, E. B.; Li, L.; Kantardjieff, K. A.; Herron, S. R.; Lim, M.; Ford, P. C. *Chem. Commun.* **2005**, 477.

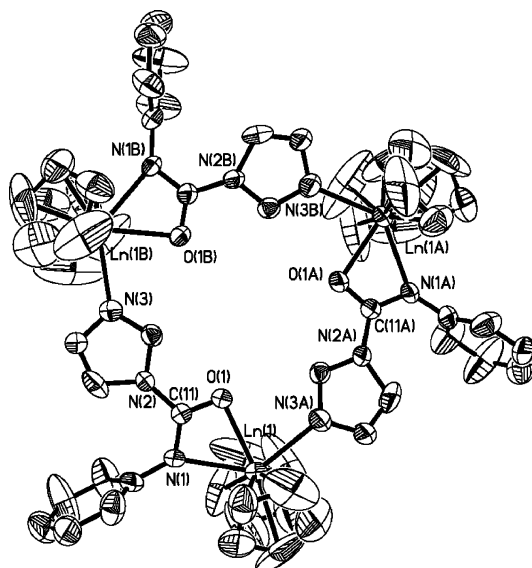


**Figure 4.** Molecular drawing and X-ray crystal structure of  $[\text{Cp}_2\text{Ln}(\mu^1,\eta^2\text{-OC(Im)NPh})_3]$  ( $\text{Ln} = \text{Yb}$  (**5**),  $\text{Dy}$  (**6**)), showing the atom-numbering scheme. Anisotropic thermal displacement ellipsoids are shown at the 30% probability level.

bonds are one of the important weak interactions in supramolecular chemistry and also play a fundamental role in the structure of DNA and the secondary and tertiary structure of proteins.<sup>17</sup> However, the inherent mechanism and role of the hydrogen bonds in solid or crystal structures are not adequately comprehended. The novel intermolecular  $\mu\text{-}\eta^2\text{-C-H}\cdots\text{O}$  hydrogen-bonding interaction should be a guest–host interaction of the THF molecules with the cavity provided in **4**.

**Reactivity of Complexes 1, 3, and 4 toward Phenyl Isocyanate.** In a previous study, we investigated insertion of organolanthanide derivatives containing the aromatic *N*-heterocycle carbazolate and pyrazolato ligands.<sup>10b</sup> The obtained information indicated that the occurrence of insertion strongly depends on the degree of steric saturation around the center metal ion and the nature of the ligands.<sup>18</sup> In order to further investigate the activity of the  $\text{Ln}-\text{N}$  bonds and ring expansion of these metallacycles, we also studied reaction of complexes **1**, **3**, and **4** with phenyl isocyanate. As shown in Scheme 2, when phenyl isocyanate was added to a THF solution of **1** and **3** at room temperature, respectively, the corresponding insertion products  $[\text{Cp}_2\text{Ln}(\mu\text{-}\eta^1\text{:}\eta^2\text{-OC(Im)NPh})_3]$  ( $\text{Ln} = \text{Yb}$  (**5**) and  $\text{Dy}$  (**6**)) were obtained, indicating that phenyl isocyanate is inserted into the  $\text{Ln}-\text{N}$  (Im) bond to construct a novel bridging ligand  $[\text{OC(Im)NPh}]$  with a  $\mu\text{-}\eta^1\text{:}\eta^2$ -bonding mode. The ligand  $[\text{OC(Im)NPh}]$  can expand the ring members from 12 to 18 in **5** or 16 to 18 in **6**. The number of metal atoms in metallacycles with  $[\text{OC(Im)NPh}]$  is independent of the lanthanide ion size; both trinuclear lanthanide macrocycles are observed in **5** and **6**. However, on treatment of phenyl

**Scheme 2**

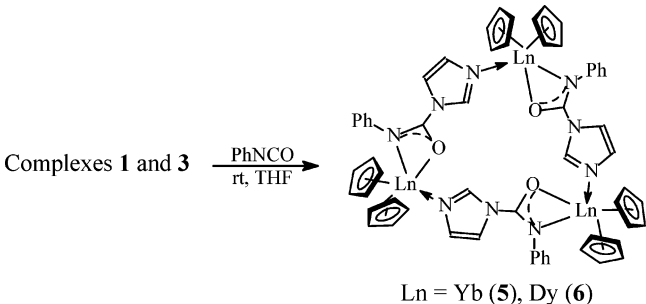


**Table 1.** Crystal and Data Collection Parameters of Complexes **2** and **3**

	<b>2</b>	<b>3</b>
formula	$\text{C}_{39}\text{H}_{39}\text{N}_6\text{Er}_3$	$\text{C}_{72}\text{H}_{92}\text{N}_8\text{O}_5\text{Dy}_4$
$M_w$	1093.54	1799.54
cryst color	pink	Pale yellow
cryst dimens (mm)	$0.20 \times 0.15 \times 0.10$	$0.15 \times 0.10 \times 0.10$
cryst syst	triclinic	triclinic
space group	$P\bar{1}$	$P\bar{1}$
unit cell dimens		
$a$ (Å)	8.291(3)	15.476(14)
$b$ (Å)	13.404(5)	16.260(15)
$c$ (Å)	18.008(7)	17.212(16)
$\alpha$ (deg)	76.802(5)	102.261(13)
$\beta$ (deg)	87.691(5)	105.411(13)
$\gamma$ (deg)	74.090(5)	115.058(12)
$V$ (Å <sup>3</sup> )	1873.2(13)	3511(6)
$Z$	2	2
$D_c$ (g·cm <sup>-3</sup> )	1.939	1.702
$\mu$ (mm <sup>-1</sup> )	6.693	4.261
$F(000)$	1038	1768
radiation ( $\lambda = 0.710730$ Å)	Mo K $\alpha$	Mo K $\alpha$
$T$ (K)	293.2	293.2
scan type	$\omega-2\theta$	$\omega-2\theta$
$\theta$ range (deg)	1.62–25.01	1.32–25.01
$h,k,l$ range	$-9 \leq h \leq 9$ $-15 \leq k \leq 15$ $-21 \leq l \leq 19$	$-18 \leq h \leq 14$ $-11 \leq k \leq 19$ $-20 \leq l \leq 19$
no. of reflns measd	7869	14 459
no. of unique reflns	6496 ( $R_{\text{int}} = 0.0266$ )	12 025 ( $R_{\text{int}} = 0.0303$ )
completeness to $\theta$	98.5% ( $\theta = 25.01$ )	97.0% ( $\theta = 25.01$ )
refinement method	full-matrix least-squares on $F^2$	full-matrix least-squares on $F^2$
data/restraints/params	6496/0/433	7505/0/469
goodness-of-fit on $F^2$	1.033	1.019
final $R$ indices	$R_1 = 0.0405$ , [ $I > 2\sigma(I)$ ]	$R_1 = 0.0587$ ,
$wR_2$	0.1072	0.1608
$R$ indices (all data)	$R_1 = 0.0538$ ,	$R_1 = 0.1086$ ,
	$wR_2 = 0.1123$	$wR_2 = 0.2097$
largest diff. peak	1.301 and -1.811	1.940 and -1.430
and hole (e·Å <sup>-3</sup> )		

isocyanate with **4**, only the original material can be obtained, indicating that PhNCO cannot insert into the  $\text{Ln}-\text{N}(\text{Tz})$  bond in **4**. This may be attributed to the bridging and chelating  $\mu\text{-}\eta^1\text{:}\eta^2$ -coordination mode of the triazolate ligand, which is disfavored for interaction of the isocyanate molecules with the central metal, thus resulting in a decrease in the  $\text{Ln}-\text{N}$  bond reactivity.

Complexes **5** and **6** have been characterized by elemental analysis and standard spectroscopic analysis, which are in good agreement with the proposed structures. In the IR spectra, the characteristic absorption at ca.  $2100$  cm<sup>-1</sup> for the  $\nu_{\text{as}}(\text{O}=\text{C}=\text{N})$  stretch of free isocyanate is absent and a new band at ca.  $1600$  cm<sup>-1</sup> attributed to the delocalized  $-\text{O}-\text{C}-\text{N}-$  stretching mode is present.<sup>12</sup> Their solid-state

(17) (a) Desiraju, G. R.; Steiner, T. R. *The Weak Hydrogen Bond in Structural Chemistry and Biology*; Oxford University Press: Oxford, 1999. (b) Lawrence, D. S.; Jiang, T.; Levett, M. *Chem. Rev.* **1995**, 95, 2229.

(18) Evans, W. J.; Fujimoto, C. H.; Ziller, J. W. *Organometallics* **2001**, 20, 4529.

**Table 2.** Crystal and Data Collection Parameters of Complexes **4–6**

	<b>4</b>	<b>5</b>	<b>6</b>
formula	C <sub>64</sub> H <sub>80</sub> N <sub>12</sub> OYb <sub>4</sub>	C <sub>60</sub> H <sub>54</sub> N <sub>9</sub> O <sub>3</sub> Yb <sub>3</sub>	C <sub>60</sub> H <sub>54</sub> N <sub>9</sub> O <sub>3</sub> Dy <sub>3</sub>
M <sub>w</sub>	1741.56	1468.24	1436.62
cryst color	red	red	pale yellow
cryst dimens (mm)	0.20 × 0.15 × 0.10	0.25 × 0.15 × 0.10	0.20 × 0.15 × 0.10
cryst syst	cubic	rhombohedral	rhombohedral
space group	I-43d	R-3	R-3
unit cell dimens			
a (Å)	27.827(3)	30.451(5)	30.575(6)
b (Å)	27.827(3)	30.451(5)	30.575(6)
c (Å)	27.827(3)	13.919(3)	13.945(4)
γ (deg)		120	120
V (Å <sup>3</sup> )	21548(4)	11178(4)	11290(4)
Z	12	6	6
D <sub>c</sub> (g·cm <sup>-3</sup> )	1.611	1.309	1.268
μ (mm <sup>-1</sup> )	5.206	3.774	2.987
F (000)	10128	4266	4194
radiation ( $\lambda = 0.710730 \text{ \AA}$ )	Mo Kα	Mo Kα	Mo Kα
T (K)	293.2	298.2	293.2
scan type	$\omega$ -2θ	$\omega$ -2θ	$\omega$ -2θ
θ range (deg)	1.79–26.00	1.65–25.01	1.65–25.01
h, k, l range	-24 ≤ h ≤ 34, -33 ≤ k ≤ 34 -34 ≤ l ≤ 33	-17 ≤ h ≤ 36 -36 ≤ k ≤ 27 -15 ≤ l ≤ 16	-28 ≤ h ≤ 36 -36 ≤ k ≤ 32 -16 ≤ l ≤ 16
no. of reflns measd	47 719	15 667	15 886
no. of unique reflns	3546 ( $R_{\text{int}} = 0.1086$ )	4378 ( $R_{\text{int}} = 0.0711$ )	4423 ( $R_{\text{int}} = 0.0459$ )
completeness to θ	99.9% ( $\theta = 26.00$ )	99.8% ( $\theta = 25.01$ )	99.8% ( $\theta = 25.01$ )
refinement method	full-matrix least-squares on $F^2$	full-matrix least-squares on $F^2$	full-matrix least-squares on $F^2$
data/restraints/params	3546/6/178	4378/0/192	4423/0/192
goodness-of-fit on $F^2$	1.083	0.970	1.133
final R indices [ $I > 2\sigma(I)$ ]	$R_1 = 0.0474$ , $wR_2 = 0.1110$	$R_1 = 0.0633$ , $wR_2 = 0.1778$	$R_1 = 0.0718$ , $wR_2 = 0.2024$
R indices (all data)	$R_1 = 0.0849$ , $wR_2 = 0.1353$	$R_1 = 0.1419$ , $wR_2 = 0.2148$	$R_1 = 0.1217$ , $wR_2 = 0.2434$
largest diff. peak and hole (e·Å <sup>-3</sup> )	1.151 and -0.448	1.402 and -0.636	1.457 and -0.654

**Table 3.** Selected Bond Lengths (Å) and Angles (deg) for **2**

Er(1)–N(1)	2.341(7)	Er(1)–C(9)	2.649(9)
Er(1)–N(3)	2.366(6)	Er(1)–C(10)	2.650(10)
Er(1)–C(6)	2.601(9)	Er(2)–N(2)	2.325(7)
Er(1)–C(4)	2.606(8)	Er(2)–N(6)	2.362(7)
Er(1)–C(3)	2.609(9)	Er(3)–N(4)	2.366(6)
Er(1)–C(5)	2.615(9)	Er(3)–N(5)	2.378(6)
Er(1)–C(1)	2.618(10)	N(1)–C(11)	1.281(14)
Er(1)–C(2)	2.619(9)	N(1)–C(13)	1.294(11)
Er(1)–C(7)	2.619(10)	N(2)–C(13)	1.299(11)
Er(1)–C(8)	2.625(10)		
N(1)–Er(1)–N(3)	88.8(2)	C(39)–N(3)–Er(1)	125.9(6)
N(2)–Er(2)–N(6)	88.0(3)	C(39)–N(4)–Er(3)	119.6(5)
N(4)–Er(3)–N(5)	85.8(2)	C(26)–N(5)–Er(3)	121.8(5)
C(13)–N(1)–Er(1)	126.6(6)	C(26)–N(6)–Er(2)	129.1(6)
C(13)–N(2)–Er(2)	124.0(6)		

structures have also been identified by X-ray single-crystal diffraction analysis. Structural analysis shows that the phenyl isocyanate molecules have inserted into the Ln–N bond ( $\mu$ -Im), forming a novel bridging ligand [OC(Im)NPh]<sup>-</sup> with a  $\mu$ -η<sup>1</sup>:η<sup>2</sup>-bonding mode. As shown in Figure 4, complex **5** is a centrosymmetric trimer in which each Yb atom connects with two [OC(Im)NPh]<sup>-</sup> units with the oxygen and nitrogen atoms from the isocyanate fragments and a nitrogen atom from another [OC(Im)NPh]<sup>-</sup> fragment. The coordination number of the center metal Yb<sup>3+</sup> is nine. Selected bond distances and angles are given in Table 6. The N(1)–C(11) and O(1)–C(11) bond lengths, 1.303(15) and 1.243(14) Å, are intermediate values between the corresponding C–N and C–O single- and double-bond distances. These bond parameters indicate substantial electronic delocalization over the O–C–N unit.<sup>19,12c</sup> Consistent with this, the Yb–N(1)

**Table 4.** Selected Bond Lengths (Å) and Angles (deg) for **3**

Dy(1)–N(8)	2.383(11)	Dy(1)–C(3)	2.701(17)
Dy(1)–N(1)	2.419(11)	Dy(2)–N(2)	2.362(11)
Dy(1)–C(7)	2.633(18)	Dy(2)–N(3)	2.489(13)
Dy(1)–O(1)	2.639(10)	Dy(3)–N(4)	2.417(11)
Dy(1)–C(8)	2.642(16)	Dy(3)–N(5)	2.462(12)
Dy(1)–C(5)	2.653(15)	Dy(4)–N(6)	2.365(11)
Dy(1)–C(9)	2.666(14)	Dy(4)–N(7)	2.392(12)
Dy(1)–C(1)	2.680(17)	N(1)–C(11)	1.351(16)
Dy(1)–C(2)	2.685(15)	N(1)–C(12)	1.403(16)
Dy(1)–C(10)	2.686(13)	N(2)–C(11)	1.368(15)
Dy(1)–C(4)	2.698(16)	N(2)–C(13)	1.393(18)
N(8)–Dy(1)–N(1)	77.6(4)	N(6)–Dy(4)–N(7)	84.1(4)
N(2)–Dy(2)–N(3)	76.4(4)	C(11)–N(1)–Dy(1)	124.4(8)
N(4)–Dy(3)–N(5)	77.9(4)	C(11)–N(2)–Dy(2)	125.1(8)

and Yb–O(1) bond distances, 2.393(11) and 2.352(8) Å, are intermediate between the values observed for the Yb–N and Yb–O single-bond distances and the Yb–N and Yb–O donor bond distances and comparable to the corresponding values found in [(C<sub>5</sub>H<sub>5</sub>)<sub>2</sub>Gd(OC(N=C(NMe<sub>2</sub>)<sub>2</sub>)NPh)]<sub>2</sub> (Gd–N 2.459(4) Å; Gd–O<sub>av</sub> 2.371(3) Å)<sup>12c</sup> if the difference in ionic radii is considered.<sup>20</sup> The structural parameters of **6** (Table 6, Figure 4) are very similar to those found in complex **5**. The complex has no unusual distances or angles in the Cp<sub>2</sub>Dy unit. The Dy–N and Dy–O distances of 2.438(12) and 2.402(9) Å are similar to the corresponding distances in complex **5** when the difference in the metal ionic radii is considered.

(19) Allen, F. H.; Kennard, O.; Watson, D. G.; Brammer, L.; Orpen, A. G. *J. Chem. Soc., Perkin Trans.* **1987**, S1.(20) Shannon, R. D. *Acta Crystallogr.* **1976**, A32, 751.

**Table 5.** Selected Bond Lengths ( $\text{\AA}$ ) and Angles (deg) for **4**

Yb(1)–N(2A)	2.287(11)	Yb(1)–C(5)	2.608(18)
Yb(1)–N(3A)	2.390(11)	Yb(1)–C(9)	2.610(18)
Yb(1)–N(1)	2.406(11)	N(1)–C(13)	1.341(15)
Yb(1)–C(3)	2.537(19)	N(1)–C(14)	1.362(16)
Yb(1)–C(4)	2.559(18)	N(2)–C(13)	1.298(15)
Yb(1)–C(11)	2.584(15)	N(2)–N(3)	1.377(14)
Yb(1)–C(2)	2.591(19)	N(2)–Yb(1B)	2.287(11)
Yb(1)–C(7)	2.591(17)	N(3)–C(14)	1.291(16)
Yb(1)–C(10)	2.597(14)	N(3)–Yb(1B)	2.390(11)
Yb(1)–C(1)	2.600(17)	O(1)…C(13)	3.317(16)
Yb(1)–C(8)	2.607(17)	O(1)…H(13A)	2.53
N(2A)–Yb(1)–N(3A)	34.2(3)	C(14)–N(1)–Yb(1)	135.2(9)
N(2A)–Yb(1)–N(1)	80.8(3)	C(13)–N(2)–N(3)	104.6(10)
N(3A)–Yb(1)–N(1)	114.8(3)	C(13)–N(2)–Yb(1B)	176.2(10)
N(2A)–Yb(1)–C(11)	110.7(7)	N(3)–N(2)–Yb(1B)	77.0(6)
N(3A)–Yb(1)–C(11)	114.4(7)	C(14)–N(3)–N(2)	106.6(10)
N(1)–Yb(1)–C(11)	77.3(4)	C(14)–N(3)–Yb(1B)	172.9(10)
C(13)–N(1)–C(14)	100.2(11)	N(2)–N(3)–Yb(1B)	68.8(6)
C(13)–N(1)–Yb(1)	124.6(8)	C(13)–H(13A)…O(1)	143.2

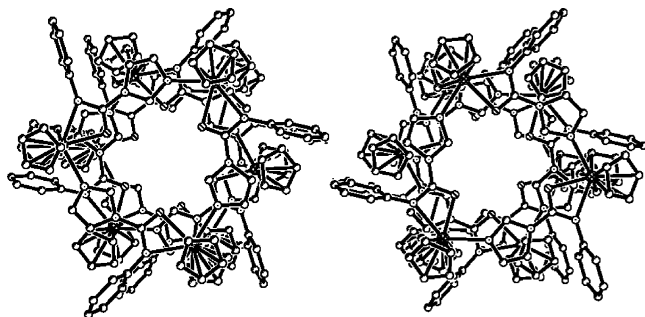
**Table 6.** Selected Bond Lengths ( $\text{\AA}$ ) and Angles (deg) for **5** and **6**

	<b>5</b> ( $\text{Ln} = \text{Yb}$ )	<b>6</b> ( $\text{Ln} = \text{Dy}$ )
Yb(1)–O(1)	2.352(8)	2.397(8)
Yb(1)–N(3A)	2.377(12)	2.434(11)
Yb(1)–N(1)	2.393(11)	2.442(10)
Yb(1)–C(7)	2.51(2)	2.61(2)
Yb(1)–C(6)	2.519(18)	2.589(18)
Yb(1)–C(3)	2.547(10)	2.566(9)
Yb(1)–C(8)	2.56(2)	2.657(19)
Yb(1)–C(4)	2.562(11)	2.564(10)
Yb(1)–C(2)	2.569(12)	2.627(12)
Yb(1)–C(10)	2.579(18)	2.616(16)
Yb(1)–C(5)	2.593(9)	2.624(8)
Yb(1)–C(1)	2.598(10)	2.658(18)
O(1)–C(11)	1.243(14)	1.254(13)
N(1)–C(11)	1.303(15)	1.276(15)
N(1)–C(17)	1.400(13)	1.378(12)
N(2)–C(20)	1.329(15)	1.325(14)
N(2)–C(11)	1.409(16)	1.434(15)
N(3)–C(20)	1.369(16)	1.309(14)
N(3)–Yb(1B)	2.377(11)	2.434(11)
O(1)–Yb(1)–N(3A)	76.7(4)	76.1(3)
O(1)–Yb(1)–N(1)	54.9(3)	54.3(3)
N(3A)–Yb(1)–N(1)	131.6(4)	130.4(3)
C(11)–O(1)–Yb(1)	95.1(8)	93.3(7)
C(11)–N(1)–Yb(1)	91.6(8)	90.7(8)
O(1)–C(11)–N(1)	118.4(12)	121.6(11)
O(1)–C(11)–N(2)	117.7(12)	115.0(10)
N(1)–C(11)–N(2)	123.9(13)	123.3(11)
O(1)–C(11)–Yb(1)	58.2(7)	59.8(6)
N(1)–C(11)–Yb(1)	60.2(7)	61.9(7)
N(2)–C(11)–Yb(1)	175.5(10)	175.5(10)

Notably, all phenyl groups orient outside the macrocycles plane, and a one-dimensional molecule pseudo-channel structure is observed in the crystal packing of **5**, as shown in Figure 5.

## Conclusion

We synthesized four novel tri- and tetranuclear lanthanide metallacycles containing bridging imidazolate and triazolate ligands, showing that both the bridge-ligand size and the lanthanide ion radii can be applied in modulation of the macrocycles. Further study on the reactivities of these complexes to isocyanate show that phenyl isocyanate readily inserts into the simple bridge  $\text{Ln}–\text{N}$  bond but cannot insert into the  $\text{Ln}–\text{N}$  bond with a  $\mu\text{-}\eta^1:\eta^2$ -bonding mode. The

**Figure 5.** One-dimension molecule pseudo-channels of complex **5**.

results demonstrate that the bonding modes of the metal–ligand bonds strongly affect insertion and reveal that insertion can be applied into ring expansions. The number of metal atoms in metallacycles with the novel bridging ligand  $[\text{OC}(\text{Im})\text{NPh}]$  is independent of the lanthanide ion size.

## Experimental Section

**General Procedures.** All operations involving air- and moisture-sensitive compounds were carried out under an inert atmosphere of purified argon or nitrogen using standard Schlenk techniques or in a glovebox. THF, toluene, and *n*-hexane were refluxed and distilled over sodium benzophenone ketyl under nitrogen immediately prior to use.  $(\text{C}_5\text{H}_5)_3\text{Ln}^{21a}$  and  $(\text{CH}_3\text{C}_5\text{H}_4)_3\text{Yb}^{21b}$  were prepared by slightly modified literature methods. Imidazole, triazole, and phenyl isocyanate were purchased from Aldrich and used without purification. Elemental analyses for C, H, and N were carried out on a Rapid CHN-O analyzer. Infrared spectra were obtained on a NICOLET FT-IR 360 spectrometer with samples prepared as Nujol mulls.

**Synthesis of  $[\text{Cp}_2\text{Yb}(\mu\text{-Im})]_3$  (1).**  $(\text{C}_5\text{H}_5)_3\text{Yb}$  (1.035 g, 2.81 mmol) and imidazole (0.192 g, 2.81 mmol) were mixed in 50 mL of THF. The solution color slowly turned from dark green to orange red in several hours. After stirring overnight at room temperature, all volatile substances were removed under vacuum to give a orange powder. Recrystallization of the powder from the solvent (THF) gave **1** as orange crystals. Yield: 0.690 g (67%). Anal. Calcd for  $\text{C}_{39}\text{H}_{39}\text{N}_6\text{Yb}_3$ : C, 42.17; H, 3.54; N, 7.57. Found: C, 42.01; H, 3.55; N, 7.68. IR (Nujol,  $\text{cm}^{-1}$ ): 3170 w, 3081 w, 1654 s, 1598 m, 1574 s, 1306 m, 1243 s, 1160 m, 1108 s, 1014 s, 960 m, 939 s, 841 m, 774 s, 663 s, 620 w.

**Synthesis of  $[\text{Cp}_2\text{Er}(\mu\text{-Im})]_3$  (2).** Following the procedure described for **1**, reaction of  $(\text{C}_5\text{H}_5)_3\text{Er}$  (0.786 g, 2.16 mmol) and imidazole (0.148 g, 2.16 mmol) gave **2** as pink crystals. Yield: 0.480 g (61%). Anal. Calcd for  $\text{C}_{39}\text{H}_{39}\text{N}_6\text{Er}_3$ : C, 42.84; H, 3.59; N, 7.69. Found: C, 42.79; H, 3.60; N, 7.77. IR (Nujol,  $\text{cm}^{-1}$ ): 3172 w, 3079 w, 1651 s, 1597 m, 1578 s, 1304 m, 1243 s, 1160 m, 1109 s, 1010 s, 960 m, 939 s, 837 m, 770 s, 662 s, 620 w.

**Synthesis of  $[\text{Cp}_2\text{Dy}(\mu\text{-Im})]_4(\text{THF})_3\cdot 2\text{THF}$  (3).** Following the procedure described for **1**, reaction of  $(\text{C}_5\text{H}_5)_3\text{Dy}$  (0.905 g, 2.53 mmol) and imidazole (0.175 g, 2.53 mmol) gave **3** as pale yellow crystals. Yield: 0.844 g (74%). Anal. Calcd for  $\text{C}_{72}\text{H}_{92}\text{N}_8\text{O}_5\text{Dy}_4$ : C, 48.06; H, 5.15; N, 6.23. Found: C, 47.68; H, 5.03; N, 6.47. IR (Nujol,  $\text{cm}^{-1}$ ): 3173 w, 3080 w, 1655 s, 1600 m, 1573 s, 1304 m, 1243 s, 1159 m, 1109 s, 1070 s, 1010 s, 939 s, 833 m, 770 s, 666 s.

(21) (a) Magin, R. E.; Manastyrskyj, S.; Dubeck, M. *J. Am. Chem. Soc.* **1963**, 85, 672. (b) Hammel, A.; Schwarz, W. H.; Weidlein, J. *J. Organomet. Chem.* **1989**, 363, C29.

**Synthesis of  $[(\text{CH}_3\text{C}_5\text{H}_4)_2\text{Yb}(\mu\text{-}\eta^1\text{:}\eta^2\text{-Tz})]_4\cdot2\text{THF}$  (4).**  $(\text{CH}_3\text{C}_5\text{H}_4)_3\text{Yb}$  (0.696 g, 1.69 mmol) and triazole (0.117 g, 1.69 mmol) were mixed in 50 mL of THF. The solution color slowly turned from dark green to orange red in several hours. After stirring overnight at room temperature, all volatile substances were removed under vacuum to give an orange powder. Recrystallization of the powder from the solvent (THF) gave **4** as orange crystals. Yield: 0.573 g (78%). Anal. Calcd for  $\text{C}_{64}\text{H}_{80}\text{N}_{12}\text{O}_2\text{Yb}_4$ : C, 44.14%; H, 4.63%; N, 9.65. Found: C, 44.06%; H, 4.57%; N, 9.74. IR (Nujol,  $\text{cm}^{-1}$ ): 3108 w, 1757 w, 1498 s, 1406 w, 1297 s, 1264 m, 1143 s, 1072 s, 1031 m, 999 s, 837 s, 774 s, 669 s, 625 w.

**Synthesis of  $[\text{Cp}_2\text{Yb}(\mu\text{-}\eta^1\text{:}\eta^2\text{-OC(Im)}\text{NPh})]_3$  (5).** To a 30 mL THF solution of **1** (0.355 g, 0.96 mmol), phenyl isocyanate (0.114 g, 0.96 mmol) was slowly added dropwise at room temperature and stirred for 12 h. The reaction solution was concentrated to ca. 3 mL by reduced pressure; yellow crystals of **5** were obtained at  $-20^\circ\text{C}$  for several days. Yield: 0.272 g (58%). Anal. Calcd for  $\text{C}_{60}\text{H}_{54}\text{N}_9\text{O}_3\text{Yb}_3$ : C, 49.08%; H, 3.70%; N, 8.59. Found: C, 48.96%; H, 3.72%; N, 8.64. IR (Nujol,  $\text{cm}^{-1}$ ): 3175 w, 1613 s, 1589 s, 1538 m, 1308 m, 1266 s, 1238 s, 1234 s, 1167 m, 1113 s, 1074 s, 1009 s, 920 s, 770 m, 735 s, 697 s, 657 w.

**Synthesis of  $[\text{Cp}_2\text{Dy}(\mu\text{-}\eta^1\text{:}\eta^2\text{-OC(Im)}\text{NPh})]_3$  (6).** Following the procedure described for **5**, reaction of **3** (0.471 g, 0.26 mmol) with phenyl isocyanate (0.125 g, 0.105 mmol) gave **6** as pale yellow crystals. Yield: 0.307 g (61%). Anal. Calcd for  $\text{C}_{60}\text{H}_{54}\text{N}_9\text{O}_3\text{Dy}_3$ : C, 50.16%; H, 3.79%; N, 8.77. Found: C, 50.09%; H, 3.82%; N, 8.92. IR (Nujol,  $\text{cm}^{-1}$ ): 3171 w, 1610 s, 1590 s, 1538 m, 1304 m, 1266 s, 1237 s, 1233 s, 1162 m, 1110 s, 1070 s, 1010 s, 918 s, 774 m, 733 s, 698 s, 658 w.

**X-ray Data Collection, Structure Determination, and Refinement.** Suitable single crystals of complexes **1–6** were sealed under argon in Lindemann glass capillaries for X-ray structural analysis. Diffraction data were collected on a Bruker SMART Apex CCD diffractometer using graphite-monochromated Mo K $\alpha$  ( $\lambda = 0.71073$

$\text{\AA}$ ) radiation. During the intensity data collection, no significant decay was observed. The intensities were corrected for Lorentz-polarization effects and empirical absorption with SADABS.<sup>22</sup> Structures were solved by direct methods using SHELXL-97.<sup>23</sup> All non-hydrogen atoms were found from the difference Fourier syntheses. The H atoms were included in calculated positions with isotropic thermal parameters related to those of the supporting carbon atoms but not included in the refinement. All calculations were performed using the SHELXL program. A summary of the crystallographic data and selected experimental information is given in Tables 1 and 2.

**$[\text{Cp}_2\text{Yb}(\mu\text{-Im})]_3$  (1).** Data on crystals of **1** was sufficient to provide atom connectivity but not high-precision metrical information due to the poor quality of data collected. Cell constants for the triclinic system, space group *P*-1 at 293(2) K, are as follows:  $a = 8.17(1)$   $\text{\AA}$ ,  $b = 13.24(2)$   $\text{\AA}$ ,  $c = 17.79(2)$   $\text{\AA}$ ,  $\alpha = 76.911(11)^\circ$ ,  $\beta = 87.722(16)^\circ$ ,  $\gamma = 74.166(16)^\circ$ ;  $V = 1802(4)$   $\text{\AA}^3$ ,  $Z = 2$ ;  $D_c = 2.047 \text{ g cm}^{-3}$ .

**Acknowledgment.** We thank the National Natural Science Foundation of China and the Research Funds of Young Teacher of Fudan University for financial support.

**Supporting Information Available:** Tables of atomic coordinates and thermal parameters, all bond distances and angles, and experimental data for all structurally characterized complexes. This material is available free of charge via the Internet at <http://pubs.acs.org>.

IC061722F

- 
- (22) Sheldrick, G. M. *SADABS, A Program for Empirical Absorption Correction*; Göttingen, Germany, 1998.  
 (23) Sheldrick, G. M. *SHELXL-97, Program for the refinement of the crystal structure*; University of Göttingen: Göttingen, Germany, 1997.